EUROPHYSICS LETTERS 31 December 1999

Europhys. Lett., **XX** (X), pp. XXX-XXX (1999)

Radial Segregation through Axial Migration

CHRISTIAN M. DURY AND GERALD H. RISTOW(*)

Fachbereich Physik, Philipps–Universität
Renthof 6, D–35032 Marburg, Germany

(received 24 February 1999; revised 13 July 1999; accepted in final form ...)

PACS. 64.75+g – Solubility, segregation, and mixing; phase separation.
PACS. 81.05Rm– Porous materials; granular materials.
PACS. 46.10+z – Mechanics of discrete systems.

Abstract. – We investigate the interplay of radial size and density segregation in a three-dimensional cylinder numerically. By fixing the size ratio of a binary particle mixture and varying the density of the smaller particle, we find a very surprising segregation dynamics in the case of a counter-balance of size segregation by density segregation. It can be best described by a "segregation wave" propagating through the system which has dissolved completely by the time it has reached the cylinder boundary.

Introduction. – The common device for mixing granular materials in industrial processing is probably a long rotating cylinder. However, when the particles differ in material properties, e.g. size or density, segregation can also occur where the final spatial distribution depends not only on the particle properties but also on the rotation speed of the cylinder [1]. In the continuous flow regime, the smaller or denser particles exhibit a fast radial segregation, forming a central region close to the rotation axis. For a long cylinder, this region leads to a core of smaller or denser particles throughout the cylinder [2] which might become unstable leading to band formation along the rotation axis [3].

Much attention has recently been focused on the radial segregation process of binary mixtures of *different particle sizes* in quasi two-dimensional rotating drums [4, 5, 6, 7] and three-dimensional cylinders [2, 8]. Individual particle trajectories were analysed and segregation parameters were defined in order to quantify the radial segregation process.

In this letter, we will direct our attention to the radial segregation process of binary mixtures of particles that differ in *density and size* which we will do numerically by means of a three-dimensional cylinder. Recent results regarding density segregation show that the initial segregation velocity scales as the logarithm of the density ratio [9], that size segregation can be partially counter-balanced by varying the particle densities at the same time [10] and that a continuum description is possible for certain cases [11]. By starting with two initial bands, we quantify the mixing of the bands and the resulting radial segregation by a normalized order parameter. Even though the final state might be well-mixed if the smaller particles are also the lighter ones, the initial inter-penetration of the two bands takes place by forming a spatially localized, segregated region, which we termed *segregation wave*.

(*) present address: Universität des Saarlandes, Institut für Theoretische Physik, D-66041 Saarbrücken, Germany

Numerical Model. – A very successful and flexible numerical technique for modelling granular materials is the Discrete Element Method (DEM); for a recent review see e.g. [12]. This method uses an explicit, constant time step to integrate Newton's second law of motion for each particle and has the ability to model in a simple way the change of geometrical contacts during collisions.

Each particle i is approximated by a sphere with radius R_i. Only contact forces during collisions are considered and the particles have the ability to rotate.

The force acting in the normal direction ($\hat{n} = \frac{\vec{r}_i - \vec{r}_j}{|\vec{r}_i - \vec{r}_j|}$) during a collision is given in our simulations as

$$F_{ij}^n = -K_n\,\delta - \gamma_n(\vec{v}_i - \vec{v}_j)\cdot\hat{n}\ ,$$

where $\delta = R_i + R_j - (\vec{r}_i - \vec{r}_j)\cdot\hat{n}$ which gives the virtual overlap of the two particles and $\vec{v}_i$ stands for the velocity of particle i. The model parameter K_n controls the stiffness of the material and is related to the Young modulus of the material, whereas γ_n stands for the dynamic damping coefficient which is related to the commonly used coefficient of restitution.

The normal force resulting from particle-wall collisions is calculated in a similar fashion by treating the wall as a particle with infinite radius and mass.

Even though a more complex contact behaviour, e.g. à la Hertz and Midlin, can be implemented in a straight-forward fashion, a linear relation is often found for small deformations and has the advantage of a constant collision time.

For the contact forces in the tangential direction, $\hat{s}$, we use viscous damping for particle-particle interactions:

$$F_s^{pp} = -\mathrm{sign}(\hat{s})\,\min(\gamma_s|\vec{v}_{ij}\cdot\hat{s}|, \mu|F_n|)$$

and static friction for particle-wall interactions:

$$F_s^{pw} = -\mathrm{sign}(\hat{s})\,\min(k_s|\int\vec{v}_{ij}\cdot\hat{s}dt|, \mu|F_n|)\ .$$

The latter leads to a static angle of repose. Values of γ_s and k_s are chosen such that the dynamic angle of repose agrees with experiment over a wide range of rotation speeds [13]. In the above equations, μ denotes the (static) Coulomb friction coefficient.

Initial Setup. – The material properties of the larger particles are chosen to correspond to the values of mustard seeds which generally show good segregation dynamics. Their diameter is 3 mm and their density $\rho_l = 1.3$ g/cm^3. The smaller particles have a diameter of 2 mm and a variable density denoted by ρ. The coefficient of restitution for particle-particle collisions is set to 0.58 and to 0.76 for particle-wall collisions. In order to save computer time, we set K_n to $8\cdot10^3$ Pa m which is about one order of magnitude softer than desired, but we checked in similar simulations that this has no effect on the investigated properties of the material, e.g. the angle of repose [13]. This gives a contact time during collisions of $8.5\cdot10^{-5}$ s. We used a total number of 13 300 particles in our simulations.

In order to have a well-defined initial configuration for binary particle mixtures, we fill the left half of the 7 cm wide and long cylinder with the smaller particles and the right half with the larger particles which is sketched in Fig. 1. The cylinder is half-filled along the rotation axis which points in the z-direction.

Segregation Order Parameter. – If a binary mixture of particles that differ in size or density is put in a rotating drum, a strong radial segregation is observed after only a few drum rotations [7]. The region occupied by the smaller or denser particles is close to the rotation

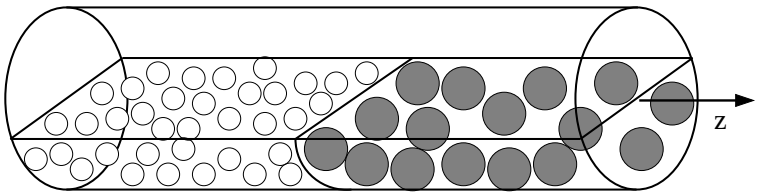

Fig. 1. – Sketch of the initial two band configuration: large (small) particles are all in the right (left) half of the cylinder and shown in gray (white).

axis and has the shape of a more or less complete circle which depends on the filling height of the cylinder. In our case of a half filling, this region can be well-approximated by a half-circle and the amount of radial segregation can be quantified by counting the percentage by volume of smaller particles in concentric rings [7, 8]. A segregation parameter $q(t, z)$, which usually shows a saturating behaviour in time to a value q_∞, can be derived by counting the deviation in the percentage by volume of smaller particles in each ring from a perfectly mixed state. The segregation parameter is normalized to one for a perfectly segregated system and we termed the value q_∞ the *final amount of segregation* which is averaged over the whole length of the drum. It is shown in Fig. 2 for our system as function of the density ratio of the smaller and larger particle components. Two regions can be distinguished clearly: (A) a very high radial segregation parameter for values of $\rho/\rho_l \geq 1$ to the right and (B) a very low radial segregation parameter for values of $\rho/\rho_l < 0.8$ to the left. In region (A), the final amount of segregation increases with density ratio until $\rho/\rho_l \approx 2$ and then it seems to decrease which is due to the fact that the core of heavier particles starts to sink into the lighter ones which is not well-captured by our segregation parameter. For more details we refer the reader to Ref. [14]. The latter region (B) corresponds to the regime where the size segregation can be counter-balanced by density segregation, as demonstrated experimentally in Ref. [10]. However, the segregation dynamics are quite different in the two regions which we will illustrate by discussing the time evolution of $q(t, z)$ in the next two sections.

Front propagation with *radial segregation (region A).* – In this case, we get a very fast radial segregation which initiates at the initial interface at $z = 0$. In Fig. 3(a), we show the time evolution of the segregation parameter q as function of position along the rotation axis for a density ratio of $\rho/\rho_l = 2$. For $t = 0$, we get $q(0, z) = 0$ throughout the system since in each of the slices where we computed q, either only large or only small particles are present and $q \equiv 0$ by definition, i.e. there is *no* radial segregation since only one particle type is present. For later times, we get a very fast radial segregation when the two particle components start to mix in the axial direction. This can be seen in Fig. 3(a) since the slope of $q(t, z)$ starts very steeply in t-direction everywhere along the rotation axis and saturates to a value of $q_\infty \approx 0.6$ throughout the system. Since the mixing starts from $z = 0$, it takes longer for particles to reach regions further away from the initial interface which explains why the increase in q starts the later the further away a region is from the initial interface.

After approximately 30 s, we find a radial core of smaller particles everywhere in the cylinder despite the fact that the concentration profile has not yet reached its steady state [14]. This was verified by visualising the central core on the computer screen. However, the particle dynamics are probably easier to illustrate for the situation when no radial segregation is observed in the steady state.

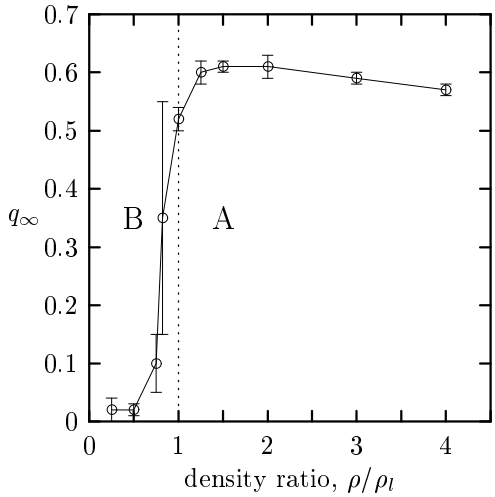

Fig. 2. – Spatially averaged final amount of segregation as function of density ratio, according to Ref. [14]. The dotted vertical line separates regions A and B, see text.

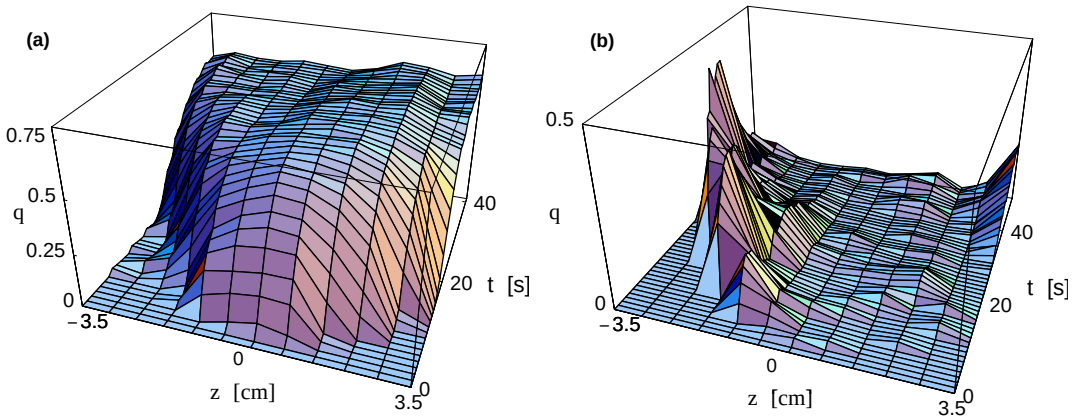

Fig. 3. – Time evolution of the radial segregation for (a) $\rho/\rho_l = 2$ and (b) $\rho/\rho_l = 0.5$.

Front propagation without *radial segregation (region B).* – For particles that only differ in size, radial segregation is observed for an arbitrarily small size difference [8]. This can be counter-balanced by making the smaller particles lighter [10]. In our case of a size ratio of 2:3, we found that the density ratio for the least radial segregation is 1:2. This gives a final value of q_∞ close to zero, see Fig. 2.

In Fig. 3(b), we show the time evolution of the segregation parameter q for a density ratio of $\rho/\rho_l = 0.5$. The picture is strikingly different from Fig. 3(a) and shows a clear wave in the segregation parameter moving to the left. We termed this new and surprising phenomena "segregation wave". This wave starts from the position of the initial front, $z = 0$, and propagates into the region initially occupied by small particles. During this process, the

amount of segregation in the region behind the wave starts to decrease. The wave reaches the cylinder end cap at a time around $t \approx 40$ s after which it dissolves completely leading to a final value of $q_\infty \approx 0$ everywhere. The origin of the wave can be understood in the following way: Since the larger particles are the denser ones, they push into the region of the smaller particles (to the left) below the free particle surface. This can be explained by different pressure values with increasing depth, resulting from the different particle densities [14].

On the other hand, no pronounced wave is visible in the right half of the cylinder, indicating that the system is always well-mixed in the region originally occupied by large particles. In this case the small particles flow in the fluidised surface layer and get directly mixed into the large ones.

In order to better visualize the spatial dynamics of this "segregation wave", we show in Fig. 4 three cross-sections along the rotation axis in the region originally occupied by small particles for three different times. Shortly after the cylinder starts to rotate, top row for $t = 1.3$ s, a core of large particles near the initial interface is clearly visible, Fig. 4(c). The core is smaller further from the interface, Fig. 4(b), and not present at all yet far away from the interface, Fig. 4(a). Also note that *no* large particles are seen close to the free surface, strongly indicating that the propagation mechanism is *not* due to surface flow but rather a pure core flow. Two cylinder revolutions later, middle row for $t = 10.3$ s, the core extends far into the left half of the cylinder, Fig. 4(d), and starts to dissolve where it was at the previous time snap shot, Figs. 4(e) & 4(f). Five revolutions later, bottom row for $t = 30.5$ *s*, the whole core has dissolved and we obtain a well-mixed state throughout the system, see Figs. 4(g), 4(h) and 4(i)).

Conclusions. – Using discrete particle simulations, we investigated the radial segregation dynamics of a binary particle mixture in a three-dimensional cylinder. The size ratio was fixed to 2:3 and we varied the density of the smaller particles in order to see the interplay of size and density radial segregation. The system was prepared to have a sharp interface of small and large particles initially. If the smaller particles also have the higher density, the radial segregation process is enhanced. On the other hand, if the smaller particles have the lower density, the radial segregation can be counter-balanced leading to a well-mixed final state. Nevertheless, the particle dynamics to reach this state are very complex and surprising in the region that was originally occupied by small particles. The large particles form a *tongue* of segregated particles in this region until they reach the boundary; then they start to mix. *No* surface flow of large particles is seen in this region which shows the possibility for other mechanisms than free surface flow to exists that can cause front advancement and segregation.

***

We would like to thank the HLRZ in Jülich and the HRZ Marburg for supporting us with a generous grant of computer time on their Cray T3E and IBM SP2, respectively. Financial support by the Deutsche Forschungsgemeinschaft is also greatfully acknowledged.

REFERENCES

[1] N. Nityanand, B. Manley, and H. Henein, *Metall. Trans. B*, **17**, 247 (1986).
[2] K. M. Hill, A. Caprihan, and J. Kakalios, *Phys. Rev. Lett.*, **78**, 50 (1997).
[3] M. Nakagawa, *Chem. Engineering Science-Shorter Communications*, **49**, 2544 (1994).
[4] E. Clément, J. Rajchenbach, and J. Duran, *Europhys. Lett.*, **30**, 7 (1995).
[5] F. Cantelaube and D. Bideau, *Europhys. Lett.*, **30**, 133 (1995).
[6] G. Baumann, I. M. Janosi, and D. E. Wolf, *Phys. Rev. E*, **51**, 1879 (1995).

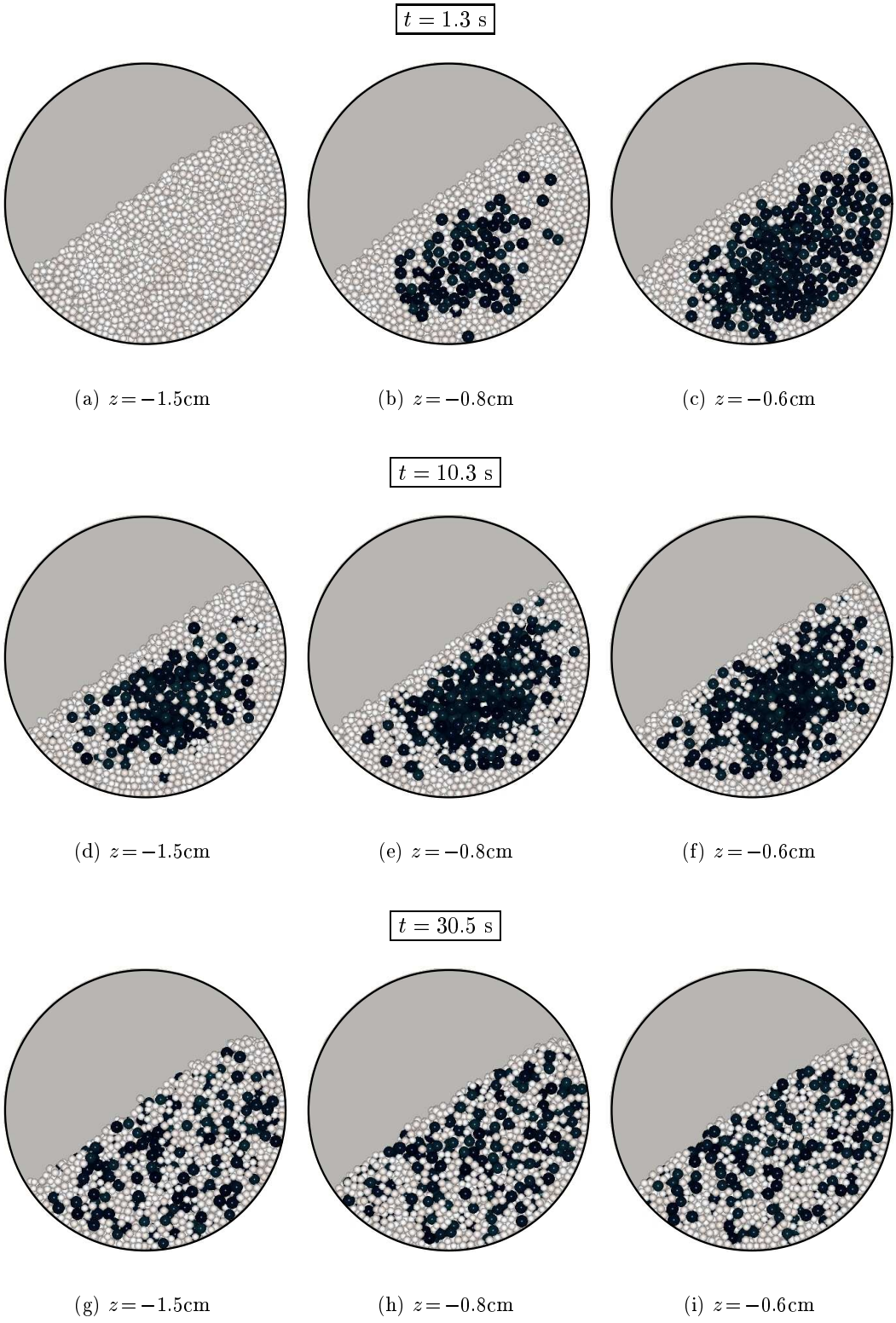

(a) $z = -1.5$cm (b) $z = -0.8$cm (c) $z = -0.6$cm

(d) $z = -1.5$cm (e) $z = -0.8$cm (f) $z = -0.6$cm

(g) $z = -1.5$cm (h) $z = -0.8$cm (i) $z = -0.6$cm

Fig. 4. – Visualisation of the core movement for $\rho/\rho_l = 0.5$.

[7] C. M. Dury and G. H. Ristow, *J. Phys. I France*, **7**, 737 (1997).
[8] C. M. Dury and G. H. Ristow, *Phys. Fluids*, **11**, 1387 (1999).
[9] G. H. Ristow, *Europhys. Lett.*, **28**, 97 (1994).
[10] G. Metcalfe and M. Shattuck, *Physica A*, **233**, 709 (1996).
[11] D. V. Khakhar, J. J. McCarthy, and J. M. Ottino, *Phys. Fluids*, **9**, 3600 (1997).
[12] G. H. Ristow, in *Annual Reviews of Computational Physics I*, edited by D. Stauffer (World Scientific, Singapore, 1994), p. 275.
[13] C. M. Dury, G. H. Ristow, J. L. Moss, and M. Nakagawa, *Phys. Rev. E*, **57**, 4491 (1998).
[14] C. M. Dury and G. H. Ristow, *Granular Matter*, **1**, 151 (1999).